Supplementary Information (SI) for Inorganic Chemistry Frontiers.

Supporting Information

Rapid synthesis and hydrothermal stability enhancement of Cu-SSZ-13 zeolites for nitrogen oxides removal

Jie Su,‡[a] Zhe Ma,‡[c] Yingzhen Wei,[b] Yida Zhou,[b] Mao Shen,[a] Shi-Bin Ren,[a] De-Man Han,[a] Mengyang Chen*[a] and Wenfu Yan*[b]

[a] School of Pharmaceutical and Chemical Engineering, Taizhou University, Taizhou, 318000, P. R. China.

[b] State Key Laboratory of Inorganic Synthesis and Preparative Chemistry, College of Chemistry, Jilin University, Changchun, 130012, P. R. China.

[c] State Key Laboratory of Heavy Oil Processing, China University of Petroleum, Qingdao, 266580, China.

Corresponding Authors

Email: mychen@tzc.edu.cn; yanw@jlu.edu.cn

Experimental Section

***Materials*:**

The following chemicals were used: N,N,N-trimethyl-1-adamantylammonium hydroxide (TMAdaOH, 25% in water, Beijing Innochem Chemical Reagent Co., Ltd), N,N-diisopropylethylamine (DIPEA, 99%, Beijing Innochem Chemical Reagent Co., Ltd), phosphoric acid (H_3PO_4, 85%, Beijing Innochem Chemical Reagent Co., Ltd), pseudo boehmite (Shanghai Macklin Biochemical Technology Co., Ltd), aluminum hydroxide ($Al(OH)_3$, 76.5% Alfa Aesar Chemical Co., Ltd), potassium hydroxide (KOH, 85wt%, Energy Chemical), sodium hydroxide (NaOH, 96%, Beijing Innochem Chemical Reagent Co., Ltd), Ludox® HS-40 colloidal silica (SiO_2, 40 wt%, Sigma-Aldrich Co., Ltd), fumed silica (SiO_2, 99.8%, Energy Chemical), copper (II) acetate monohydrate ($Cu(CH_3COO)_2{\cdot}H_2O$, 98 wt.%, Beijing Innochem Chemical Reagent Co., Ltd). All materials were used as received without further purification.

Synthesis of SAPO-18 seed:

2.65 g of pseudo boehmite and 4.15 g of phosphoric acid were added to 17.38 g of deionized (DI) water and stirred for 2 h. Afterwards, 4.14 g of N, N-diisopropylethylamine (DIPEA) was introduced, and the mixture was stirred for another 1 h. After adding 0.48 g of fumed silica, the mixture was stirred for an additional hour. The resulting suspension was transferred into a 25 mL Teflon-lined stainless-steel autoclave and heated at 160 °C for 8 d. The product was centrifuged, washed several times with DI water, and dried at 80 °C overnight. The as-synthesized SAPO-18 zeolite was used as a seed without calcination.

Synthesis of SSZ-13 zeolites:

SSZ-13 zeolites with varying Si/Al ratios, $TMAda^+$/Si ratios, seed content, and crystallization times were synthesized hydrothermally. Typically, 0.43 g of NaOH, 0.2 g of KOH, and 0.3 g of $Al(OH)_3$ were dissolved in 7.9 g of DI water. Then, 0.5 g of TMAdaOH and 0.216 g of SAPO-18 seed were added, and the mixture was stirred for 2 h. Afterward, 3.6 g of silica sol (HS-40) was introduced,

followed by another 2 h stirring. The final synthesis mixture had the composition Al_2O_3: 16 SiO_2: 2 KOH: 7 NaOH: 0.4 TMAdaOH: 302 H_2O: seed (15 wt.%). The mixture was transferred into a 25 mL autoclave and subjected to hydrothermal synthesis at 160 °C for 0–30 h, depending on the desired crystallization time. The resulting product was centrifuged, washed with DI water, and dried overnight at 80 °C. To vary the Si/Al ratios, the amount of $Al(OH)_3$ was adjusted between 0.1 and 0.4 g, while the TMAdaOH content was varied between 0.25 and 1.0 g to achieve different $TMAda^+$/Si ratios. Seed content (5–20 wt.% relative to the theoretical zeolite yield) was also adjusted to study its effect on SSZ-13 synthesis.

Synthesis of conventional SSZ-13 (SSZ_{conv}-13) zeolites:

SSZ_{conv}-13 was synthesized by a conventional hydrothermal method. Typically, 0.2 g of NaOH, 0.125 g of $Al(OH)_3$, and 4 g of TMAdaOH were dissolved in 7.15 g of DI water and stirred for 1 h. Afterwards, 1.5 g of silica sol was added, followed by 2 h of stirring. The molar composition of the final mixture was Al_2O_3: 16 SiO_2: 8 NaOH: 7.6 TMAdaOH: 835 H_2O. The mixture was transferred into a 25 mL autoclave and heated at 160 °C for 4 d. The product was centrifuged, washed with DI water, and dried overnight at 80 °C, followed by calcination at 600 °C for 8 h (Yield: ~60%).

***Ion exchange and hydrothermal aging treatment*:**

Cu-SSZ-13 and Cu-SSZ_{conv}-13 zeolites were prepared via two-step ion-exchanged process. For Cu-SSZ-13, the as-synthesized SSZ-13 zeolite was ion-exchanged twice with 1 M NH_4Cl at 80 °C to remove Na^+ and K^+ ions, forming NH_4-SSZ-13. Copper ions were introduced by ion-exchange with a 0.004 M $Cu(CH_3COO)_2$ solution at 70 °C for 2 h. The zeolite slurries were then filtered, washed with DI water, and dried at 80 °C overnight, and calcined at 550 °C for 6 h to remove the OSDA and NH_4^+. For Cu-SSZ_{conv}-13, the SSZ_{conv}-13 zeolite was first calcined at 600 °C for 8 h before being exchanged with NH_4Cl and $Cu(CH_3COO)_2$, followed by calcination at 500 °C for 5 h.

To prepare CuCe-SSZ-13, 1 g of Cu-SSZ-13 was mixed with varying

amounts of cerium(III) nitrate hexahydrate (0.015 g, 0.030 g, 0.060 g) or ceric(IV) nitrate (0.014 g, 0.028 g, 0.056 g), followed by grinding. The mixtures were calcined at 750 °C for 4 h using a solid-state ion-exchange method. Zeolitic catalysts with different Ce loadings were denoted as $CuCe(III)_{0.5}$-SSZ-13, $CuCe(III)_{1.0}$-SSZ-13, $CuCe(III)_{2.0}$-SSZ-13, $CuCe(IV)_{0.5}$-SSZ-13, $CuCe(IV)_{1.0}$-SSZ-13, $CuCe(IV)_{2.0}$-SSZ-13, and $CuCe(III)_{0.5}Ce(IV)_{0.5}$-SSZ-13 where the numbers of 0.5, 1.0, and 2.0 present Ce content.

To investigate hydrothermal stability, the catalysts were aged in flowing air containing 10 vol.% H_2O at 800 °C for 8 h.

Characterization:

The crystallinity and phase purity of the samples were characterized by X-ray diffraction (XRD) using Cu K_α radiation (λ = 1.5418 Å) on a Rigaku D-Max 2550 diffractometer. The relative crystallinity was evaluated by comparing the sum of peak intensity (2θ = 9.7°, 16.3°,17.8°, 20.9°, 24.9°, 25.9°, 31.1° and 31.6°). Scanning electron microscopy (SEM) images were measured with JEOL S-4800. Transmission electron microscopy (TEM) images and elemental mapping images were recorded on a Thermo Scientific Talos F200i. Nitrogen adsorption/desorption characterization of samples was performed at 77 K after degassing at 350 °C under vacuum using a Micromeritics 2020 analyzer. Ultraviolet-visible diffuse reflectance spectra (UV-Vis DRS) of the samples in the 200–800 nm range were obtained on a U-4100 at the ambient temperature. Ammonia temperature-programmed desorption (NH_3-TPD) testing of samples was performed using a Micromeritics AutoChemII 2920 automated chemical adsorption analysis unit under helium flow using a thermal conductivity detector (TCD). The hydrogen temperature-programmed reduction (H_2-TPR) tests were performed on an AutoChemII 2920 analyzer. Samples were pretreated at 550°C for 1 h in an Ar atmosphere (25 mL min^{-1}) and then TPR tests were performed in 10% H_2 / Ar at a flow rate of 10 mL min^{-1} from 40 to 825 °C at 10 °C min^{-1}. X-ray photoelectron spectroscopy (XPS) spectra were tested using a Thermo ESCALAB 250 spectrometer under monochromatic Al K_α excitation.

^{27}Al NMR tests were performed on Bruker Avance Neo 600 MHz WB spectrometer with BBO MAS probe operating at a magnetic field strength of 14.1 T.

***Catalytic testing*:**

SCR of NO_x was conducted in a fixed-bed quartz reactor with an inner diameter of 6 mm. The catalyst (0.1 g, 40–60 mesh) was placed in the reactor, and the test reaction conditions were as follows.

500 ppm NO, 500 ppm NH_3, 5% O_2, 5% H_2O, with N_2 as the balance gas at a total flow rate of 500 mL/min, corresponding to a gaseous hourly space velocity (GHSV) of 200,000 h^{-1}. Inlet and outlet gas compositions were monitored in real time using FTIR spectrometer (MKS, MultiGas 2030HS). NO conversion was calculated as follows:

$$\text{NO conversion} = \left(1 - \frac{[NO]_{out} + [NO_2]_{out}}{[NO]_{in} + [NO_2]_{in}}\right) \times 100\%$$

Figures and Tables

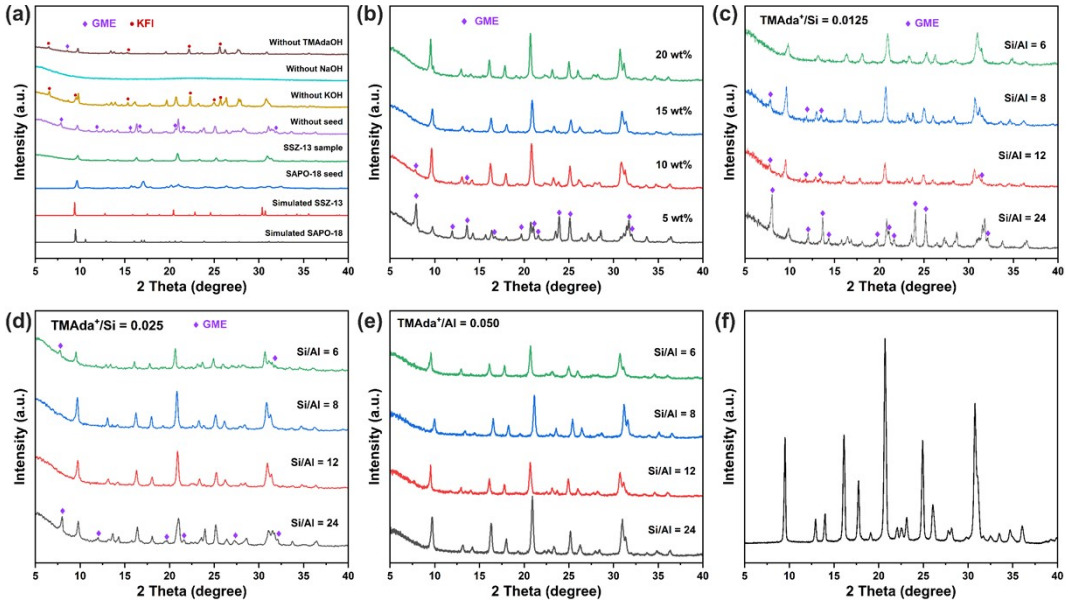

Fig. S1 XRD patterns of (a) simulated SAPO-18, simulated SSZ-13 and as-synthesized samples under various synthesis systems. XRD patterns of as-synthesized samples (b) with different seed contents, (c) at $TMAda^+$/Si ratio of 0.0125, (d) at $TMAda^+$/Si ratio of 0.025 and (e) at $TMAda^+$/Si ratio of 0.050. (f) XRD pattern of conventional SSZ_{conv}-13 zeolite crystallized at 120 h.

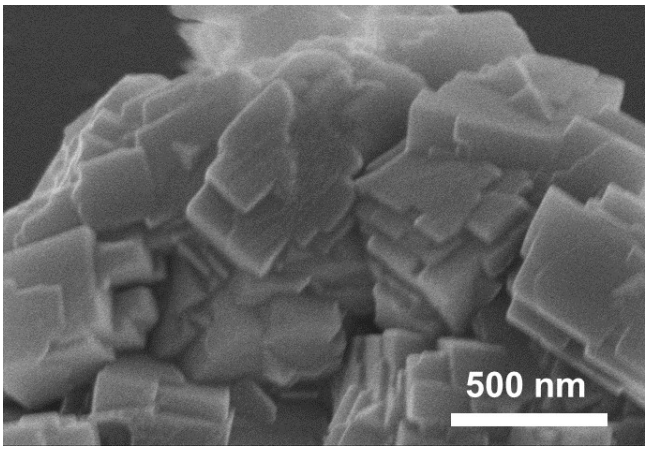

Fig. S2 SEM images of SSZ-13 zeolite crystallized at 6 h.

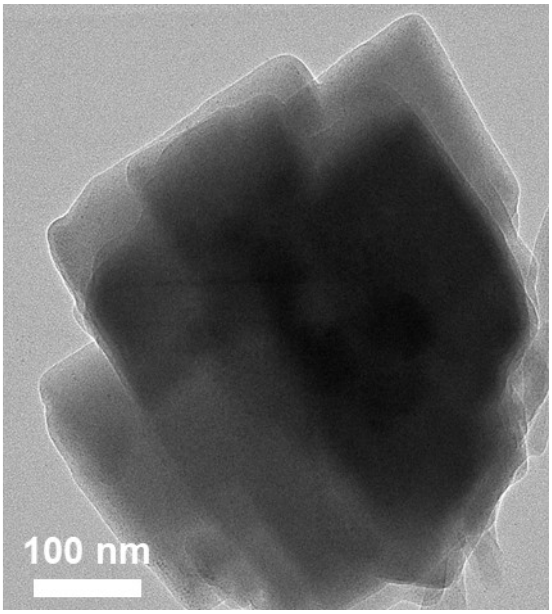

Fig. S3 TEM image of SSZ-13 zeolite crystallized at 6 h.

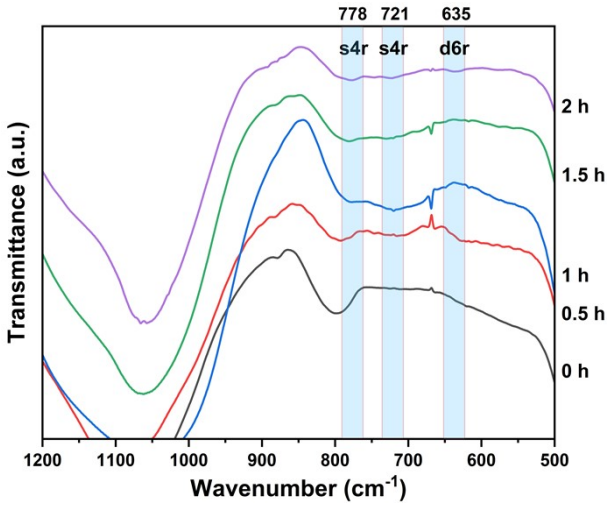

Fig. S4 FTIR spectra of the samples throughout the hydrothermal crystallization period of 0–2 h.

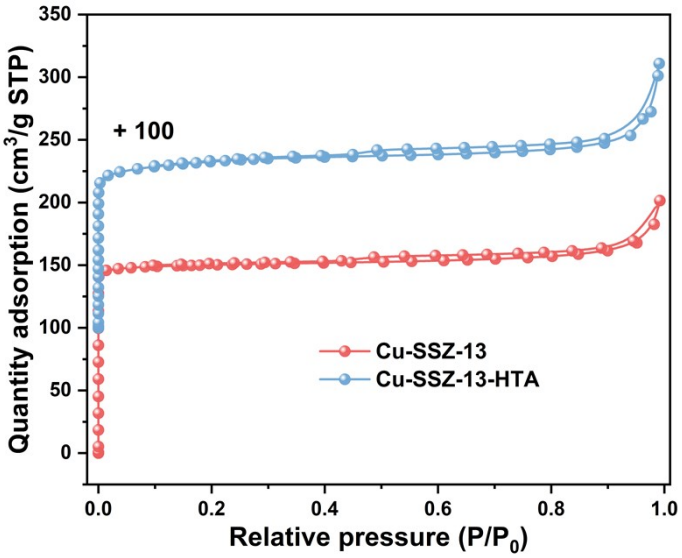

Fig. S5 Nitrogen adsorption-desorption isotherms of Cu-SSZ-13 and Cu-SSZ-13-HTA zeolites.

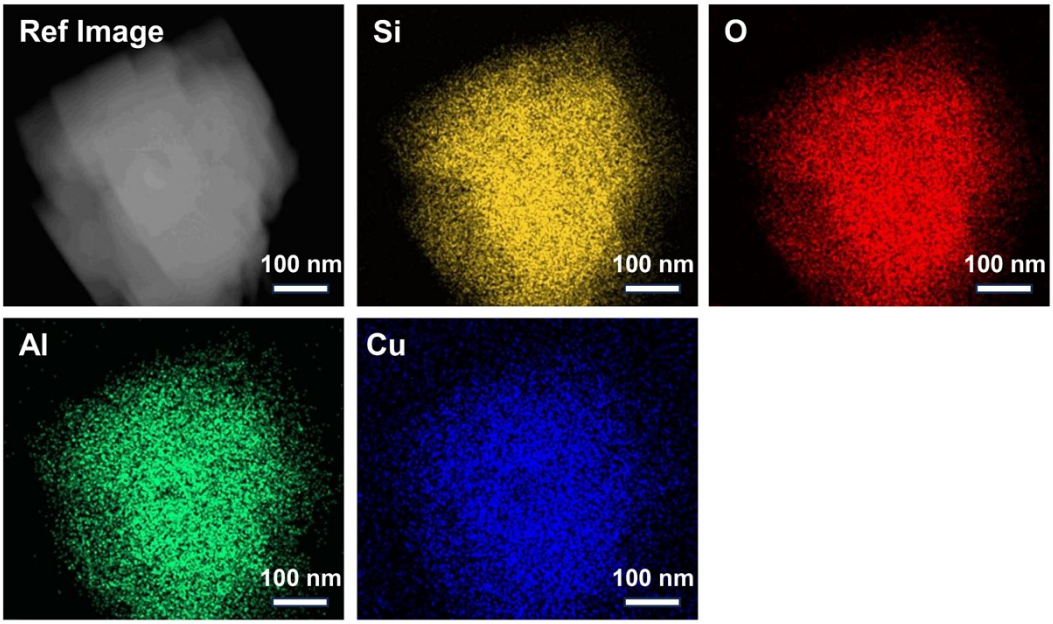

Fig. S6 Elemental mapping images of Cu-SSZ-13.

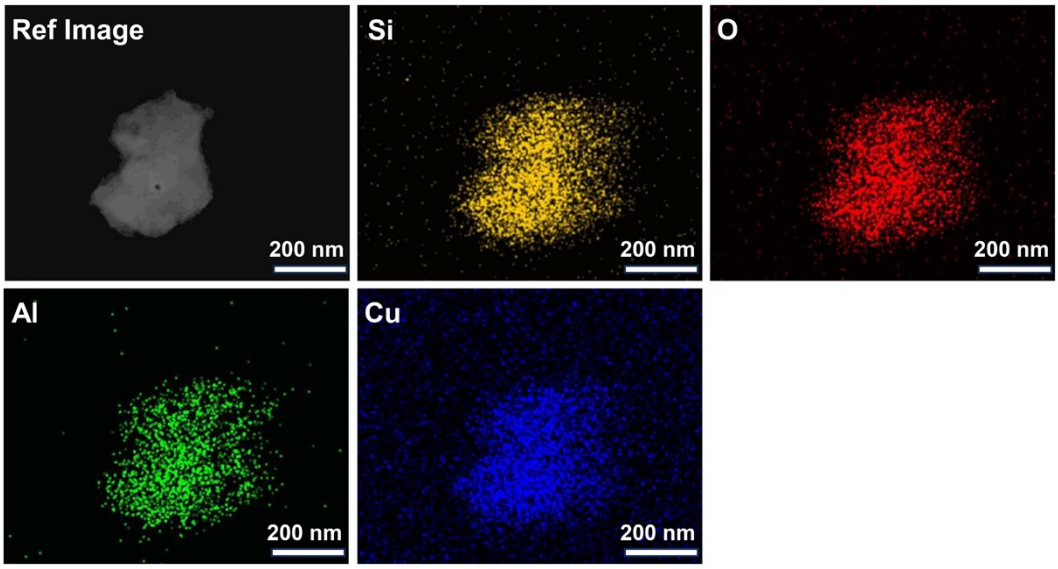

Fig. S7 Elemental mapping images of Cu-SSZ-13-HTA.

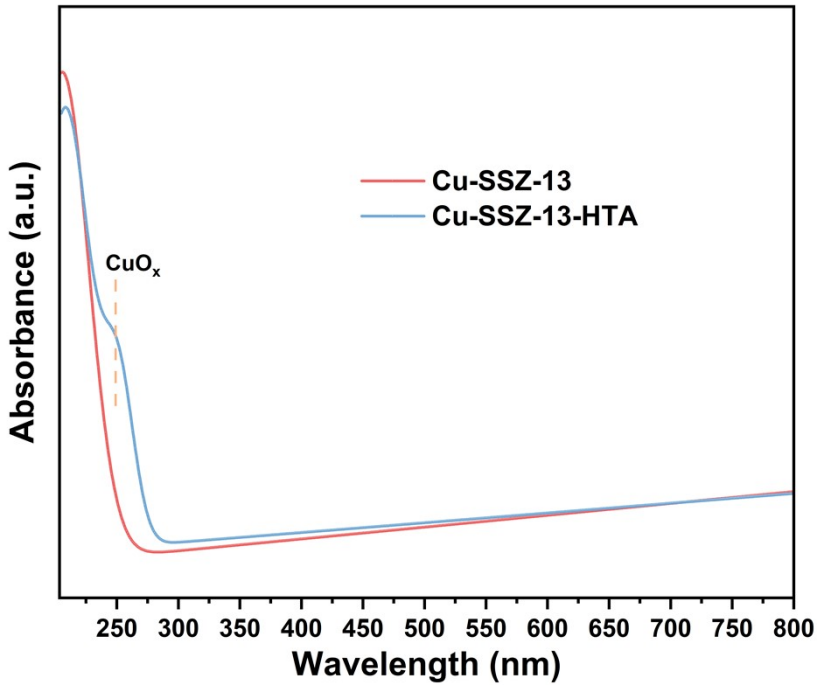

Fig. S8 UV-vis DRS spectra of Cu-SSZ-13 and Cu-SSZ-13-HTA zeolites.

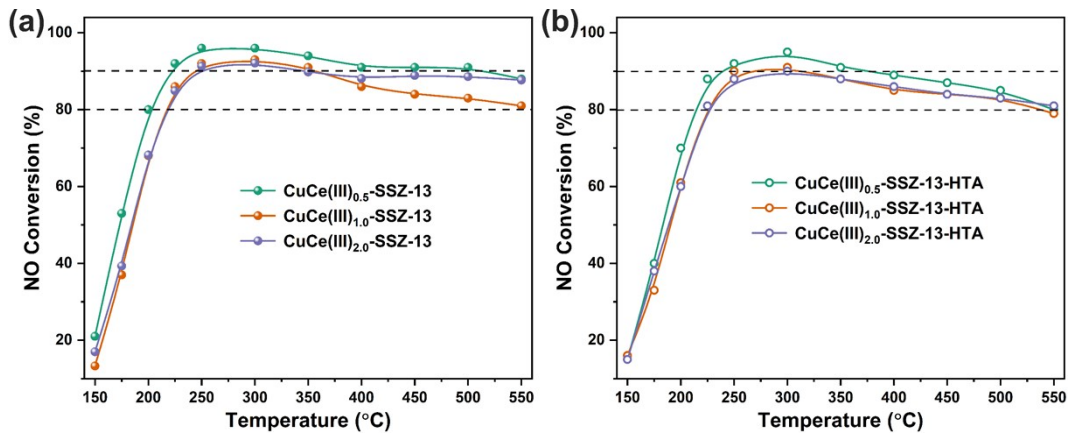

Fig. S9 NO conversion as a function of temperature for CuCe(III)-SSZ-13 zeolites with different Ce(III) content. Reaction conditions: 500 ppm NO, 500 ppm NH_3, 5% O_2, and 5% H_2O, balanced with N_2 at a GHSV of 200,000 h^{-1}.

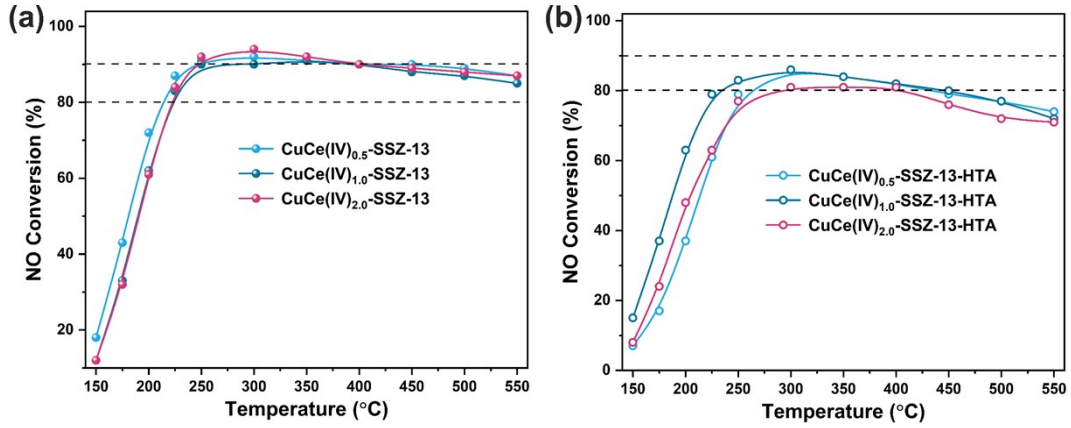

Fig. S10 NO conversion as a function of temperature for CuCe(IV)-SSZ-13 zeolites with different Ce(IV) content. Reaction conditions: 500 ppm NO, 500 ppm NH_3, 5% O_2, and 5% H_2O, balanced with N_2 at a GHSV of 200,000 h^{-1}.

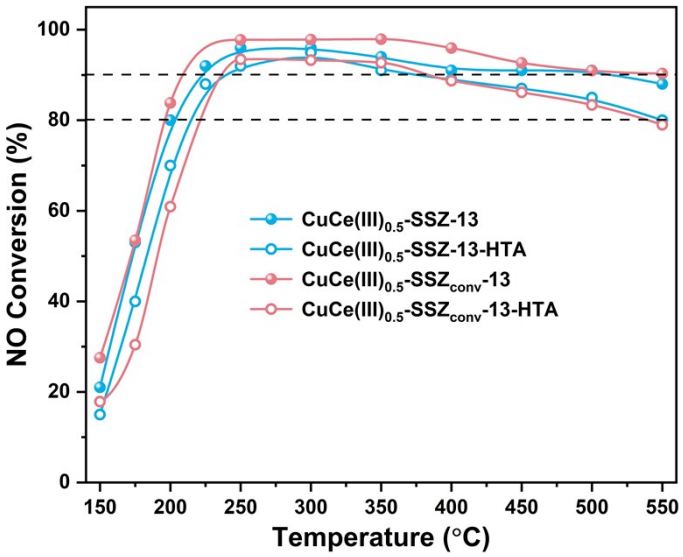

Fig. S11 NH_3-SCR performance comparison between $CuCe(III)_{0.5}$-SSZ-13 and $CuCe(III)_{0.5}$-SSZ_{conv}-13.

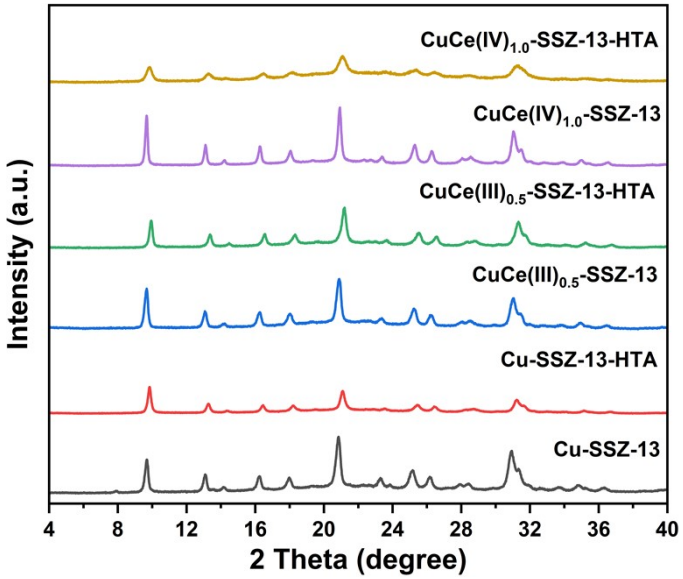

Fig. S12 XRD patterns of Cu-SSZ-13 and CuCe-SSZ-13 zeolites.

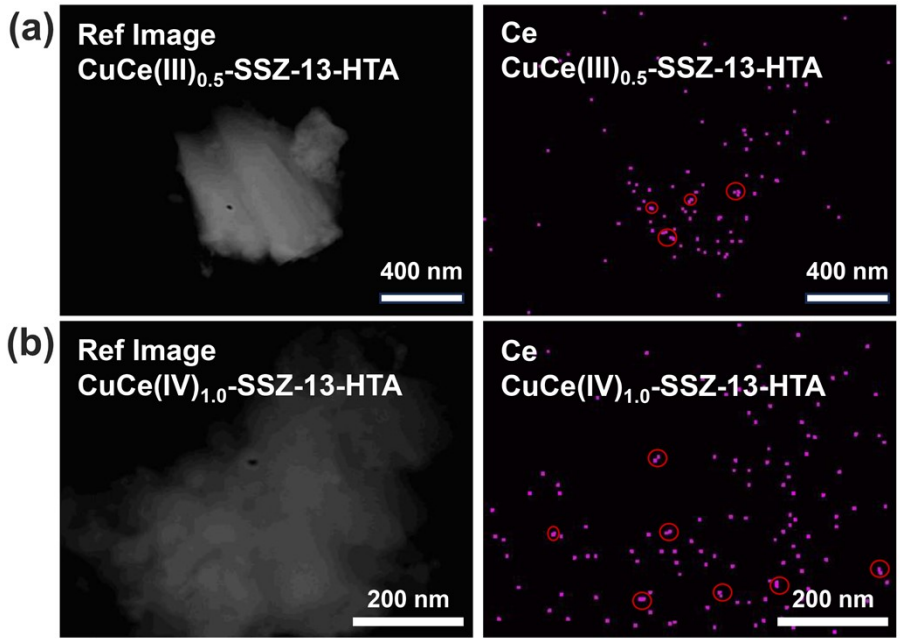

Fig. S13 Elemental mapping images of (a) $CuCe(III)_{0.5}$-SSZ-13-HTA and (b) $CuCe(IV)_{1.0}$-SSZ-13-HTA.

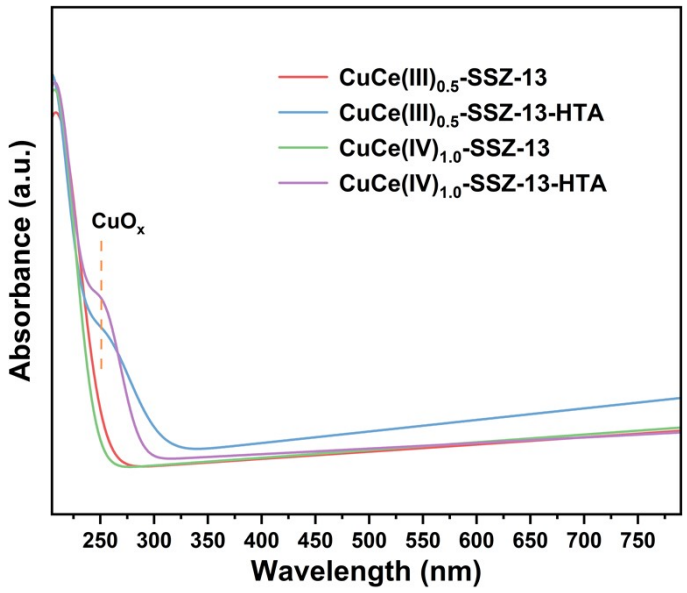

Fig. S14 UV-vis DRS spectra of $CuCe(III)_{0.5}$-SSZ-13 and $CuCe(IV)_{1.0}$-SSZ-13 zeolites.

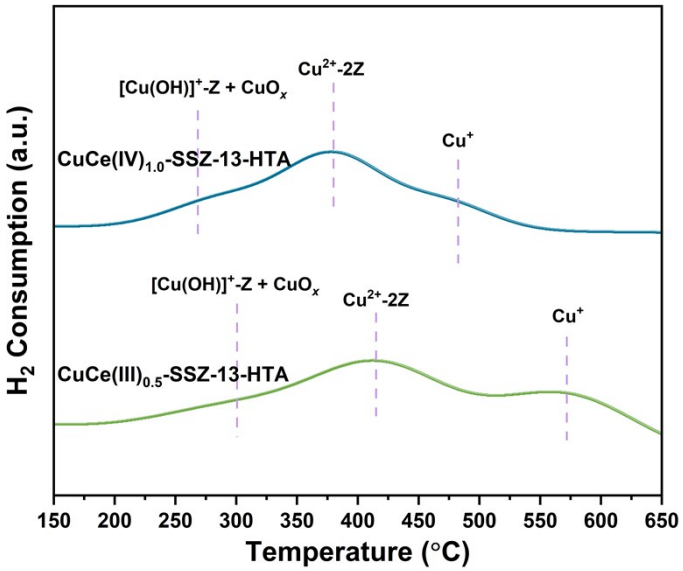

Fig. S15 H_2-TPR profiles of $CuCe(III)_{0.5}$-SSZ-13-HTA and $CuCe(IV)_{1.0}$-SSZ-13-HTA.

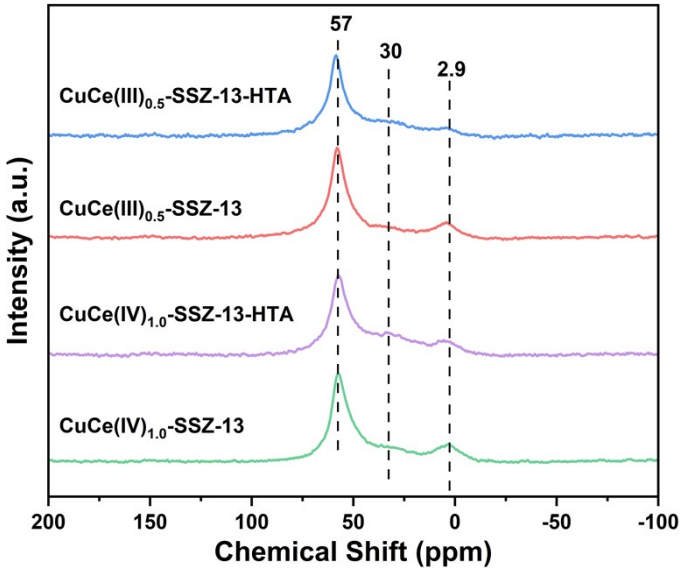

Fig. S16 ^{27}Al MAS NMR spectra of $CuCe(III)_{0.5}$-SSZ-13 and $CuCe(IV)_{1.0}$-SSZ-13 before and after hydrothermal ageing.

Table S1. Comparison of crystallization times between SSZ-13 synthesized using SAPO-18 seeds in this study and SSZ-13 synthesized with various seeds in previous reports.

Sample	Seed Type	Crystallization Conditions	Reference
SSZ-13	SAPO-34	155 °C, 5 d	Ref 1
SSZ-13	SSZ-13	100-120 °C, 2-6 d	Ref 2
SSZ-13-$TP_{0.03}$	SSZ-13	150 °C, 4 d	Ref 3
CHA-type zeolite	SSZ-13	170 °C, 20 rpm, 1 d	Ref 4
High-silica **CHA**-type aluminosilicates	SSZ-13	170 °C, 40 rpm, 2 d	Ref 5
CC-SS-Seed	SSZ-13	140 °C, 3 d	Ref 6
SSZ-13-CA-S-6h	SSZ-13	160 °C, 6 h	Ref 7
STM-24	SSZ-13	120 °C, 24 h	Ref 8
SSZ-13	SSZ-13	160 °C, 5 d	Ref 9
SSZ-13	SAPO-18	160 °C, 6 h	This work

Table S2. Chemical compositions of Cu-SSZ-13 and Cu_{conv}-SSZ-13.

Sample	Si/Al[a]	Cu/Al[a]
Cu-SSZ-13	4.5	0.15
Cu_{conv}-SSZ-13	6.0	0.15

[a] Measured by inductively coupled plasma (ICP).

Table S3. Texture properties of Cu-SSZ-13 and Cu-SSZ-13-HTA.

Sample	S_{BET} ($m^2\ g^{-1}$)[a]	V_{micro}($cm^3\ g^{-1}$)[b]
Cu-SSZ-13	626	0.23
Cu-SSZ-13-HTA	522	0.14

[a] S_{BET} (total surface area) calculated by applying the BET equation. [b] V_{micro} (micropore area) calculated using the *t*-plot method.

Reference

1 H. Zhao, Y. Zhao, Y. Ma, X. Yong, M. Wei, H. Chen, C. Zhang and Y. Li, Enhanced hydrothermal stability of a Cu-SSZ-13 catalyst for the selective reduction of NO_x by NH_3 synthesized with SAPO-34 micro-crystallite as seed, *J. Catal.,* 2019, **377**, 218–223.

2 X. Zhang, T. Dou, Y. Wang, J. Yang, X. Wang, Y. Guo, Q. Shen, X. Zhang and S. Zhang, Green synthesis of Cu-SSZ-13 zeolite by seed-assisted route for effective reduction of nitric oxide, *J. Cleaner Prod.,* 2019, **236**, 117667.

3 H. Zhang, Q. An, F. Yu and B. Fan, Seed-assisted synthesis of a nanosheet-assembled
hierarchical SSZ-13 zeolite by coupling a small amount of TMAdaOH with TPOAC, *New J. Chem.,* 2024, **48**, 8352–8360.

4 H. Imai, N. Hayashida, T. Yokoi and T. Tatsumi, Direct crystallization of CHA-type zeolite from amorphous aluminosilicate gel by seed-assisted method in the absence of organic-structure-directing agents, *Microporous Mesoporous Mater.,* 2014, **196**, 341–348.

5 R. Osuga, M. Yabushita, T. Matsumoto, M. Sawada, T. Yokoi, K. Kanie and A. Muramatsu, Fluoride-free synthesis of high-silica CHA-type aluminosilicates by seed-assisted aging treatment for starting gel, *Chem. Commun.,* 2022, **58**, 11583–11586.

6 X. Wang, R. Zhang, H. Wang and Y. Wei, Strategy on effective synthesis of SSZ‐13 zeolite aiming at outstanding performances for NH_3‐SCR process, *Catal. Surv. Asia,* 2020, **24**, 143–155.

7 Q. Li, W. Cong, J. Zhang, C. Xu, F. Wang, D. Han, G. Wang and L. Bing, Rapid synthesis of hierarchical nanosized SSZ-13 zeolite with excellent MTO catalytic performance, *Microporous Mesoporous Mater.,* 2022, **331**, 111649.

8 H. Zhang, Q. Dong, P. Shan, D. Pan, B. Fan and R. Li, Synthesis of highly crystallized SSZ-13 with a small amount of organic structure-directing agent in the presence of seeds, *Microporous Mesoporous Mater.,* 2021, **324**, 111287.

9 Z. Xu, H. Ma, Y. Huang, W. Qian, H. Zhang and W. Ying, Synthesis of submicron SSZ-13 with tunable acidity by the seed-assisted method and its performance and coking behavior in the MTO reaction, *ACS Omega,* 2020, **5**, 24574−2458.